Brazilian Journal
of Chemical
Engineering

ISSN 0104-6632
Printed in Brazil

Vol. 20, No. 04, pp. 375 - 390, October - December 2003

# EXPERIMENTAL ANALYSIS AND EVALUATION OF THE MASS TRANSFER PROCESS IN A TRICKLE-BED REACTOR

J.D.Silva[2*], F.R.A.Lima[1] C.A.M.Abreu[2] and A.Knoechelmann[2]

[1]Nuclear Energy Department, Federal University of Pernambuco (UFPE), Phone (081) 3271-8251,
Fax (081) 3271-8250, Av. Prof. Luiz Freire 1000, 50740-540, Recife - PE, Brazil.
[2]Chemical Engineering Department, Federal University of Pernambuco (UFPE), Phone (081) 3271-8236,
Fax (081) 3271-3992, R. Prof. Artur de Sá, 50740-521, Recife - PE Brazil.
E-mail: jornandesdias@yahoo.com.br

*(Received: January 26, 2002 ; Accepted: May 29, 2003)*

**Abstract** - A transient experimental analysis of a three-phase descendent-cocurrent trickle-bed $H_2O/CH_4$-$Ar/\gamma$-$Al_2O_3$ system was made using the stimulus-response technique, with the gas phase as a reference. Methane was used as a tracer and injected into the argon feed and the concentration vs time profiles were obtained at the entrance and exit of the bed, which were maintained at 298K and 1.013 $10^5$ Pa. A mathematical model for the tracer was developed to estimate the axial dispersion overall gas-liquid mass transfer and liquid-solid mass transfer coefficients. Experimental and theoretical results were compared and shown to be in good agreement. The model was validated by two additional experiments, and the values of the coefficients obtained above were confirmed.
*Keywords*: trickle-bed, mass transfer, three-phase reactor, methane gas tracer, transient.

## INTRODUCTION

Analysis of the response of a system to an input disturbance is a well-established technique for studying the mixing characteristics of many types of equipment. This type of procedure referred to as the study of dynamic processes has been applied to, for example, heat exchangers, distillation columns and chemical reactors (Silva et al.,1999, 2000a,b; Lamine et al., 1996; Tsamatsoulis and Papayannakos, 1995; Ramachandran and Chaudhari, 1983; Iliuta et al., 1997; Iliuta et al., 1999).

Trickle-bed reactors with cocurrent downflow of the gaseous and liquid phases have been utilized in several catalytic processes (Ramachandran and Smith, 1979; Silva, 1996; Al-Dahhan et al., 1997; Attou et al., 1999; Chin and King, 1999; Funk et al., 1990; Gallezot et al., 1998; Iliuta et al., 1997; Jiang et al., 1999). These reactors can be used in the development of chemical processes such as catalytic hydrodesulfurization, production of calcium acid sulfite, oxidation of formic acid in water, synthesis of butynediol, production of sorbitol, hydrogenation of aniline to cyclohexylaniline and oxidation of sulfur dioxide on activated carbon (Larachi et al., 1991; Burghardt et al., 1990; Burghardt et al., 1995; Gianetto and Specchia, 1992; Latifi et al., 1997; Pawelec et al., 2001; Pironti et al., 1999; Rajashekharam et al., 1998; Wu et al., 1996; Reinecke et al., 1998).

Three-phase reactions in these reactors may be limited by effects related to the availability of the surface of the catalyst to the gas. In trickle-bed reactors these restrictions may be attributed to gas solubility, mixing in the liquid phase or gas-liquid and liquid-solid mass transfer limitations.

Mathematical modeling of these three-phase reactors may involve the mechanisms of forced

*To whom correspondence should be addressed

convection, axial dispersion, interphase mass transport, intraparticle diffusion, adsorption and chemical reaction. Normally, these models are constructed relating each phase to the others.

In pioneering work Ramachandran and Smith (1979), proposed a plug-flow model to describe the adsorption and reaction of the gas on the catalytic surface. In this work an axial dispersion model for the liquid phase, which involves only the effects of adsorption is reported. Emphasis was placed upon evaluation, of parameters $D_{ax}$, $K_{GL}$ and $k_{LS}$, the mixing and mass transfer coefficients of the gas component.

## MATHEMATICAL MODEL

The theoretical model described here is one-dimensional and based upon the concentration of the gas tracer in the gas, liquid, and solid phases during cocurrent operation (Silva et al., 2000a; Burghardt et al., 1990; Ramachandran and Smith, 1979; Iliuta et al., 2002). The model adopted for the gas tracer within these phases is constrained by the following simplifications: (i) the system is isothermal; (ii) the gas phase is modeled as a plug flow; (iii) the liquid phase is modeled taking axial dispersion into account; (iv) the system operates with partial wetting of the bed; (v) there is intraparticle diffusion in the pores of the spherical catalytic particle; (vi) rapid adsorption equilibrium is achieved in the system; (vii) the system operates with a small concentration of the tracer in order to minimize disturbances to reactor conditions.

Based on these simplifications, the mass balance equations that describe the transient behavior of this system are given by the following coupled partial differential equations:

$$H_{d,G}\frac{\partial C_G(z,t)}{\partial t}+V_{SG}\frac{\partial C_G(z,t)}{\partial z}= -K_{GL}a_{GL}\left[HC_G(z,t)-C_L(z,t)\right] \quad (1)$$

$$H_{d,L}\frac{\partial C_L(z,t)}{\partial t}+V_{SL}\frac{\partial C_L(z,t)}{\partial z} = D_{ax}\frac{\partial^2 C_L(z,t)}{\partial z^2} +K_{GL}a_{GL}\left[HC_G(z,t)-C_L(z,t)\right] -f_e k_{LS}a_P\left[C_L(z,t)-C_r(R,t)\big|_{\forall t}\right] \quad (2)$$

$$H_S(1+\rho_P K_A)\frac{\partial C_r(r,t)}{\partial t}=\frac{D_e}{r^2}\frac{\partial}{\partial r}\left[r^2\frac{\partial C_r(r,t)}{\partial r}\right] \quad (3)$$

The initial and boundary conditions for the above equations are respectively

Equation 1:

$$C_G(z,)\big|_{\forall z}=0 \;;\; C_G(0,t)\big|_{\forall t}=C_{G,0} \quad (4)$$

Equation 2:

$$C_L(z,0)\big|_{\forall z}=0;$$

$$\frac{\partial C_L(0,t)}{\partial z}\bigg|_{\forall t}=\frac{V_{SL}}{D_{ax}}C_L(0,t)\big|_{\forall t}; \quad (5)$$

$$\frac{\partial C_L(L,t)}{\partial z}\bigg|_{\forall t}=0$$

Equation 3:

$$C_r(r,0)\big|_{\forall r}=0;\ \frac{\partial C_r(0,t)}{\partial r}\bigg|_{\forall t}=0;\qquad \frac{\partial C_r(R,t)}{\partial r}\bigg|_{\forall t}=\frac{k_{LS}}{D_e}\left[C_L(z,t)-C_r(R,t)\big|_{\forall t}\right] \quad (6)$$

The superficial velocities in Eqs. 1 and 2 may be determined from the following empirical models: superficial velocity of the liquid phase (Hutton et al., 1974):

$$V_{SL}=\frac{H_{d,L}^3\rho_L g}{2\mu_L a_{GL}^2}\ \frac{\cos^2\beta}{\left(H_S+H_{d,L}\right)^2} -\delta_{GL}\left[\frac{H_{d,L}^3}{3\mu_L a_{GL}^2}\frac{\cos^2\beta}{\left(H_S+H_{d,L}\right)^3}+\frac{H_{d,L}^2\cos^3\beta}{2\mu_L a_{GL}^2}\frac{\left(1-H_S-H_{d,L}\right)}{\left(H_S+H_{d,L}\right)^3}\right] \quad (7)$$

where $\delta_{GL}$ is given by

$$\delta_{GL}=\left[\frac{8.5\mu_G a_P^2 G_G}{\rho_G}+\frac{a_P G_G^2}{\rho_G}\left(\frac{\mu_G a_P}{G_G}\right)^{0.1}\right]\frac{1}{\left(1-H_S-H_{d,L}\right)^3} \quad (8)$$

superficial velocity of the gaseous phase (Specchia and Baldi, 1977):

$$\delta_{GL} = K_1 \frac{\left[1-\left(1-H_S-H_{d,G}\right)\right]^2}{\left(1-H_S-H_{d,G}\right)^3}\mu_G V_{SG} + K_2 \frac{\left[1-\left(1-H_S-H_{d,G}\right)\right]}{\left(1-H_S-H_{d,G}\right)^3}\rho_G V_{SG}^2) \quad (9)$$

Equations 1 to 3 and their initial and boundary conditions can be analyzed with dimensionless variable terms from the following ratios:

$$\Gamma_G(\xi,t_A)=\frac{C_G(z,t)}{C_{G,0}};\ \Gamma_L(\xi,t_A)=\frac{C_L(z,t)}{C_{G,0}H};$$

$$\Gamma_r(\eta,t_A)=\frac{C_r(r,t)}{C_{G,0}H};\ t_A=\frac{V_{SG}t}{H_{d,G}L};\quad \xi=\frac{z}{L};\ \eta=\frac{r}{R} \quad (10)$$

Thus, Eqs. 1 to 3 are rewritten as

$$\frac{\partial\Gamma_G(\xi,t_A)}{\partial t_A}+\frac{\partial\Gamma_G(\xi,t_A)}{\partial\xi} + \alpha\Gamma_G(\xi,t_A)=\alpha\Gamma_L(\xi,t_A) \quad (11)$$

$$\frac{\partial\Gamma_L(\xi,t_A)}{\partial t_A}+\kappa\frac{\partial\Gamma_L(\xi,t_A)}{\partial\xi}-\frac{1}{P_E^*}\frac{\partial^2\Gamma_L(\xi,t_A)}{\partial\xi^2} = \gamma\Gamma_G(\xi,t_A)-\gamma\Gamma_L(\xi,t_A) - \vartheta\left[\Gamma_L(\xi,t_A)-\Gamma_r(1,t_A)\big|_{\forall t}\right] \quad (12)$$

$$\frac{\partial\Gamma_r(\eta,t_A)}{\partial t_A}=\frac{\lambda}{\eta^2}\frac{\partial}{\partial\eta}\left[\eta^2\frac{\partial\Gamma(\eta,t_A)}{\partial\eta}\right] \quad (13)$$

The dimensionless initial and boundary conditions for Eqs. 11, 12 and 13 are given by

$$\Gamma_G(\xi,0)\big|_{\forall\xi}=0;\quad \Gamma_G(0,t_A)\big|_{\forall t_A}=1 \quad (14)$$

$$\Gamma_L(\xi,0)\big|_{\forall\xi}=0;\ \frac{\partial\Gamma_L(0,t_A)}{\partial\xi}\bigg|_{\forall t_A}=P_E\Gamma_L(0,t_A)\big|_{\forall t_A};\quad \frac{\partial\Gamma_L(1,t_A)}{\partial\xi}\bigg|_{\forall t_A}=0 \quad (15)$$

$$\Gamma_r(\eta,0)\big|_{\forall\eta}=0;\ \frac{\partial\Gamma_r(0,t_A)}{\partial\eta}\bigg|_{\forall t_A}=0;\quad \frac{\partial\Gamma_r(1,t_A)}{\partial\eta}\bigg|_{\forall t_A}=Sh\left(\Gamma_L(\xi,t_A)-\Gamma_r(1,t_A)\big|_{\forall t_A}\right) \quad (16)$$

The dimensionless parameters in Eqs. 11 to 16 are defined as

$$\alpha=\frac{K_{GL}a_{GL}LH}{V_{SG}};\ \kappa=\frac{V_{SL}H_{d,G}}{V_{SG}H_{d,L}};\quad \gamma=\frac{K_{GL}a_{GL}LH_{d,G}}{V_{SG}H_{d,L}};\ \vartheta=\frac{f_e\ a_p\ k_{LS}\ L\ H_{d,G}}{H_{d,L}\ V_{SG}} \quad (17)$$

$$P_E^*=\frac{V_{SG}\ L}{D_{ax}}\frac{H_{d,L}}{H_{d,G}};\quad \lambda=\frac{D_e\ H_{d,G}\ L}{R^2H_S(1+\rho_P K_A)V_{SG}};\quad Sh=\frac{k_{LS}R}{D_e};\ P_E=\frac{V_{SL}\ L}{D_{ax}} \quad (18)$$

## SOLUTION OF SYSTEM EQUATIONS

The partial differential equation system defined by Eqs. 11 to 13 may be solved in the Laplace domain, as reported in previous studies (Silva et al., 2000b; Iliuta et al.,1999; Burghardt et al., 1995; Ramachandran and Smith, 1979).

$$s\Gamma_G^*(\xi,s)+\frac{d\Gamma_G^*(\xi,s)}{d\xi}+\alpha\Gamma_G^*(\xi,s)=\alpha\Gamma_L^*(\xi,s) \quad (19)$$

$$s\Gamma_L^*(\xi,s)+\kappa\frac{d\Gamma_L^*(\xi,s)}{d\xi}-\frac{1}{P_E^*}\frac{d^2\Gamma_L^*(\xi,s)}{d\xi^2} = \gamma\Gamma_G^*(\xi,s)-\gamma\Gamma_L^*(\xi,s) - \vartheta\left[\Gamma_L^*(\xi,s)-\Gamma_r^*(1,s)\right] \quad (20)$$

$$s\Gamma_r^*(\eta,s)=\frac{\lambda}{\eta^2}\frac{\partial}{\partial\ \eta}\left[\eta^2\frac{\partial\Gamma_r^*(\eta,s)}{\partial\eta}\right] \quad (21)$$

The boundary conditions in the Laplace domain are defined by

$$\Gamma_G^*(0,s)=1/s \quad (22)$$

$$\frac{d\,\Gamma_L^*(0,s)}{d\xi} = P_E\,\Gamma_L^*(0,s);\quad \frac{d\,\Gamma_L^*(1,s)}{d\xi} = 0 \tag{23}$$

$$\frac{d\Gamma_r^*(1,s)}{d\eta} = Sh\left[\Gamma_L^*(\xi,s) - \Gamma_r^*(1,s)\right];$$
$$\frac{d\Gamma_r^*(0,\ s)}{d\eta} = 0 \tag{24}$$

To find the relationship between $\Gamma^*_L(\xi, s)$ in the liquid phase and $\Gamma^*_r(1, s)$ at the outer surface of the catalyst particle, Eq. 21 was solved with the boundary conditions in Eqs. 24 (Appendix A).

$$\Gamma_r^*(1,s) = \frac{Sh\ \Gamma_L^*(\xi,s)}{\left\{\left[\phi(s)\right]\cot gh\left[\phi(s)\right] + Sh - 1\right\}};$$
$$\left[\phi(s)\right]^2 = \frac{s}{\lambda} \tag{25}$$

Eq. 25 was introduced in to Eq.20 and Eqs. 19 and 20 were rearranged as

$$\frac{d\,\Gamma_G^*(\xi,s)}{d\xi} + a_1(s)\Gamma_G^*(\xi,s) = \alpha\,\Gamma_L^*(\xi,s) \tag{26}$$

$$\frac{1}{P_E^*}\frac{d^2\Gamma_L^*(\xi,\ s)}{d\xi^2} - \kappa\frac{d\,\Gamma_L^*(\xi,s)}{d\xi}$$
$$+\nu(s)\,\Gamma_L^*(\xi,s) = -\gamma\,\Gamma_G^*(\xi,s) \tag{27}$$

where

$$R(s) = \frac{\left[\phi(s)\right]\cot gh\left[\phi(s)\right] - 1}{\left\{\left[\phi(s)\right]\cot gh\left[\phi(s)\right] + Sh - 1\right\}};$$
$$\nu(s) = \left[s + \gamma + \vartheta R(s)\right];\ a_1(s) = (s + \alpha) \tag{28}$$

Combining Eqs. 26 and 27 gave two third-order linear ordinary differential equations with constant coefficients for $\Gamma^*_G(\xi, s)$ and $\Gamma^*_L(\xi, s)$:

$$\frac{d^3\Gamma_G^*(\xi,s)}{d\xi^3} + \delta(s)\frac{d^2\Gamma_G^*(\xi,s)}{d\xi^2}$$
$$-K_1(s)\frac{d\Gamma_G^*(\xi,s)}{d\xi} + K_2(s)\,\Gamma_G^*(\xi,s) = 0 \tag{29}$$

and

$$\frac{d^3\Gamma_L^*(\xi,s)}{d\xi^3} + \delta(s)\frac{d^2\Gamma_L^*(\xi,s)}{d\xi^2}$$
$$-K_1(s)\frac{d\Gamma_L^*(\xi,s)}{d\xi} + K_2(s)\,\Gamma_L^*(\xi,s) = 0 \tag{30}$$

where

$$K_2(s) = \left[\alpha\gamma - a_1(s)\nu(s)\right]P_E^*;$$
$$K_1(s) = \left[a_1(s)\kappa + \nu(s)\right]P_E^*; \tag{31}$$
$$\delta(s) = \left[a_1(s) - P_E^*\kappa\right]$$

The formal solutions for Eqs. 29 and 30 were suggested by Ramachandran and Smith (1979) and were applied here in the following forms:

$$\Gamma_G^*(\xi,s) = \sum_{i=1}^{3} f_i(s)\exp\left[\lambda_i(s)\right]\xi;$$
$$\Gamma_L^*(\xi,s) = \sum_{i=1}^{3}\left[\lambda_i(s) - a(s)\right]\frac{f_i(s)}{\alpha}\exp\left[\lambda_i(s)\right]\xi \tag{32}$$

where

$$\lambda_1(s) = J(s) + T(s) - \frac{1}{3}\delta(s);$$
$$\lambda_2(s) = -\frac{1}{2}\left[J(s) + T(s)\right] - ;$$
$$-\frac{1}{3}\delta(s) + \frac{\sqrt{3}}{2}i\left[J(s) - T(s)\right] \tag{33}$$

$$\lambda_3(s) = -\frac{1}{2}\left[J(s) + T(s)\right]$$
$$-\frac{1}{3}\delta(s) - \frac{\sqrt{3}}{2}i\left[J(s) - T(s)\right] \tag{34}$$

and

$$H(s) = -\left\{\frac{9\delta(s)\,K_1(s) + 27K_2(s) + 2\left[\delta(s)\right]^3}{54}\right\};$$
$$J(s) = \left\{H(s) + \sqrt{\left[Q(s)\right]^3 + \left[H(s)\right]^2}\right\}^{1/2} \tag{35}$$

$$Q(s) = -\left\{\frac{3K_1(s) + \left[\delta(s)\right]^2}{9}\right\};$$
$$T(s) = \left\{H(s) - \sqrt{\left[Q(s)\right]^3 + \left[H(s)\right]^2}\right\}^{1/2} \quad (36)$$

The boundary conditions, Eqs. 22 and 23, were used to obtain the integration constants of Eq 32 (Appendix C), so, the response for the gas tracer in the gaseous phase was given by

$$\Gamma_G^*(\xi,s) = \frac{D_1(s)}{D(s)}\exp\lambda_1\xi + \frac{D_2(s)}{D(s)}\exp\lambda_2\xi + \frac{D_3(s)}{D(s)}\exp\lambda_3\xi \quad (37)$$

Determinants $D_1(s)$, $D_2(s)$ and $D_3(s)$ were introduced in to Eq. 37 (Appendix C), resulting in

$$\Gamma_G^*(\xi,s) = \frac{\Gamma_G^*(0,s)}{D(s)}\left\{\left[V_1^*\left(\lambda_2(s),\lambda_3(s),a_1(s)\right)\exp\lambda_1(s)\,\xi + V_2^*\left(\lambda_1(s),\lambda_3(s),a_1(s)\right)\exp\lambda_2(s)\xi + V_3^*\left(\lambda_1(s),\lambda_2(s),a_1(s)\right)\exp\lambda_3(s)\xi\right]\right\} \quad (38)$$

where $V_1^*$, $V_2^*$and $V_3^*$ are functions defined in the Laplace domain and are given in Appendix C.

For $\xi = 1$ it was possible to obtain the response of the gas tracer at the exit of the fixed bed with Equation 39:

$$\Gamma_G^*(1,s) = \int_{\xi=0}^{\xi=1}\Gamma_G^*(\xi,s)\,\delta(\xi-1)\,d\xi \quad (39)$$

Thus

$$\Gamma_G^*(1,s) = \frac{\Gamma_G^*(0,s)}{D(s)}\left\{\left[V_1^*\left(\lambda_2(s),\lambda_3(s),a_1(s)\right)\exp\lambda_1(s) + V_2^*\left(\lambda_1(s),\lambda_3(s),a_1(s)\right)\exp\lambda_2(s) + V_3^*\left(\lambda_1(s),\lambda_2(s),a_1(s)\right)\exp\lambda_3(s)\right]\right\} \quad (40)$$

The transfer function of the system was defined by the ratio of the exit function to the entrance function [$G^*(1, s) = \Gamma^*_G(1, s)/ \Gamma^*_G(0, s)$]**,** so the final transfer function was

$$G_G^*(1,s) = \frac{1}{D(s)}\left\{\left[V_1^*\left(\lambda_2(s),\lambda_3(s),a_1(s)\right)\exp\lambda_1(s) + V_2^*\left(\lambda_1(s),\lambda_3(s),a_1(s)\right)\exp\lambda_2(s) + V_3^*\left(\lambda_1(s),\lambda_2(s),a_1(s)\right)\exp\lambda_3(s)\right]\right\} \quad (41)$$

The theoretical concentration at the exit of the fixed bed, $\Gamma_G(1,t_A)_k^{Calc}$, was calculated by the convolution of the experimental concentrations $\Gamma_G^{Exp}$ (iω) with $G_G^*(1, i\omega)$. $\Gamma_G(1,t_A)_k^{Calc}$ was obtained by numerical inversion, using the numerical fast Fourier transform (FFT) algorithm (Cooley and Twkey, 1965) that changed the time domain according to following equation**:**

$$\left[\Gamma_G(1,t_A)\right]_k^{Calc} = TF^{-1}\left[\Gamma_E^{Exp}(i\,\omega) * G_G^*(1,i\omega)\right] \quad (42)$$

where the Laplace variable (s) was substituted by iω in the Fourier domain.

## MATERIALS AND EXPERIMENTAL METHODOLOGY

To study the axial dispersion and the mass transfer effects**,** a three-phase gas-liquid-solid reactor was mounted according to Fig 1. The assembled system consisted of a fixed bed with a height of 0.16

m and an inner diameter of 0.03 m; catalytic particles were contacted by a cocurrent gas-liquid downward flow. Experiments were conducted under conditions such that the superficial velocities of the gas and liquid phases were maintained within the trickle-bed regime (Ramachandran and Chaudhari, 1983) $V_{SL}$ in the range of $10^{-4}$ m $s^{-1}$ to 3 $10^{-3}$ m $s^{-1}$ and $V_{SG}$ in the range of 2 $10^{-2}$ m $s^{-1}$ to 45 $10^{-2}$ m $s^{-1}$.

The gas phase (4% volume Ar +$CH_4$), flowing downward cocurrently in contact with 70.00g of the solid bed ($\gamma$-$Al_2O_3$, CGO-70, Rhone-Poulenc), was continuously measured using a thermal conductivity detector (TCD) coupled to an AD/DA interface. The tracer was turned on and off at differing superficial velocities; deviations in the signal from its baseline, negative steps, provided a measurement of its concentration versus time at the entrance and exit of the bed.

The methodologies applied to evaluate the axial dispersion and the mass transfer parameters for the $CH_4$ – Ar – $H_2O$ / $\gamma$-$Al_2O_3$ system were the following:

- analysis of the negative - step curves at the entrance and exit of the bed;
- residence time distribution (RTD); determination by the method of moments applied to the normalized curves. A comparison of experimental results with the expressions obtained from the transfer function ($G_G^*(1,s)$; Eq.41) as developed for this system;
- evaluation of the model parameters ($D_{ax}$, $K_{GL}$, $k_{LS}$) used as initialization values when obtained by the method of moments;
- optimization of the model parameters by comparing the calculated values of concentration with the experimental data.

To calculate the concentrations within this numerical model, several numerical values for the $CH_4$–Ar–$H_2O$ / $\gamma$-$Al_2O_3$ system are required; in Table 1 these values, obtained under similar experimental conditions, are listed (Silva, 1996).

Performance of the trickle-bed is affected by many factors, such as interphase mass transfer, intraparticle diffusion, axial dispersion, gas and liquid holdup and partial wetting. These factors are incorporated into this model. As the liquid flow was maintained constant, Silva's tabulated values representing liquid holdup ($H_{d,L}$) and partial wetting (fe) (1996) were adopted.

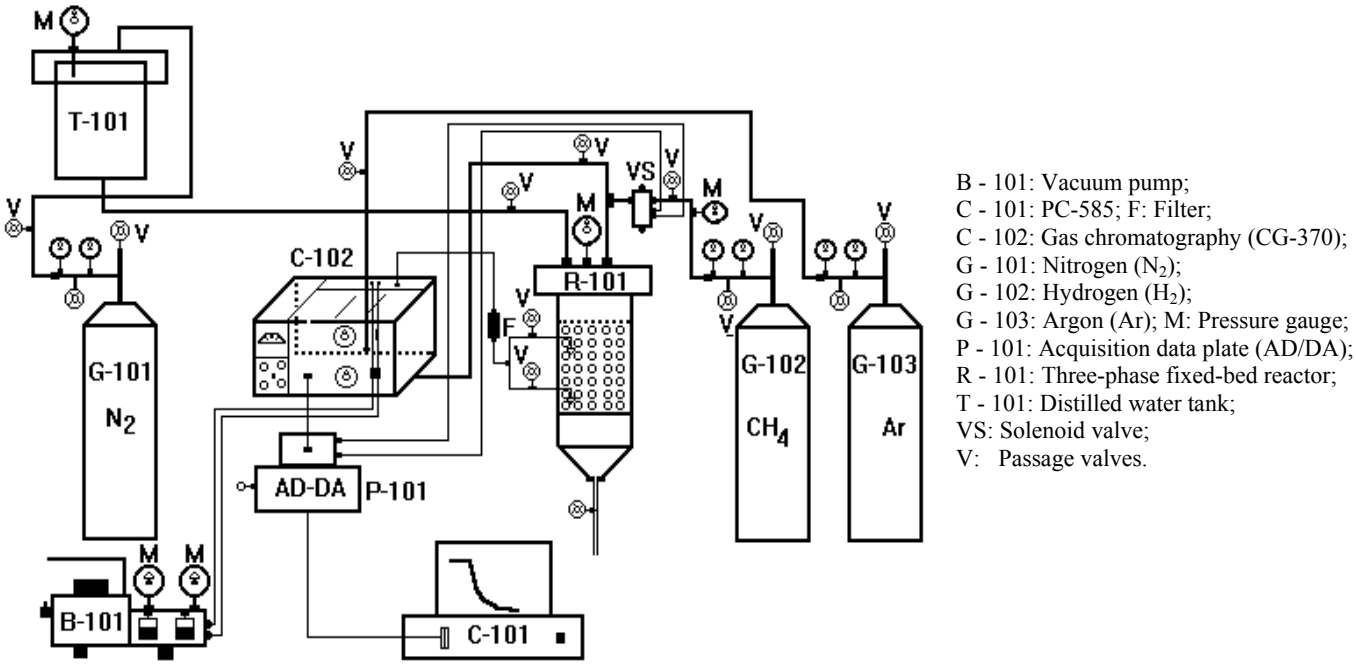


**Figure 1:** Experimental Setup

**Table 1: Properties, parameters and operational variables for the $H_2O/Ar\text{-}CH_4/\gamma\text{-}Al_2O_3$ system (Silva, 1996).**

| Numerical Values | | | | | |
|---|---|---|---|---|---|
| $\mu_L$, kg m$^{-1}$ s$^{-1}$ | 8.91 10$^{-4}$ | $V_{SG}$, m s$^{-1}$ | 29.46 10$^{-3}$ | R, m | 1.60 10$^{-3}$ |
| $\mu_G$, kg m$^{-1}$ s$^{-1}$ | 1.23 10$^{-5}$ | $V_{SL}$, m s$^{-1}$ | 1.91 10$^{-4}$ | $\sigma_L$, kg s$^{-2}$ | 7.22 10$^{-2}$ |
| $\rho_L$, kg m$^{-3}$ | 1.01 10$^{3}$ | $a_{GL}$, m$^2$ m$^{-3}$ | 8.13 10$^{4}$ | $f_e$ | 3.50 10$^{-1}$ |
| $\rho_G$, kg m$^{-3}$ | 6.63 10$^{-1}$ | $a_P$, m$^2$ m$^{-3}$ | 1.14 10$^{3}$ | H | 5.70 10$^{-2}$ |
| $\delta_{GL}$, kg m$^{-2}$ s$^{-2}$ | 1.14 10$^{1}$ | $K_A$, m$^3$ kg$^{-1}$ | 6.45 10$^{-4}$ | $D_e$, m$^2$ s$^{-1}$ | 4.56 10$^{-3}$ |
| $\rho_P$, kg m$^{-3}$ | 3.15 10$^{3}$ | L, m | 1.60 10$^{-1}$ | $\varepsilon_{ex}$ | 3.90 10$^{-1}$ |
| $H_{d,G}$ | 2.00 10$^{-1}$ | $D_P$, m | 3.20 10$^{-3}$ | W, kg | 7.00 10$^{-2}$ |
| $H_{d,L}$ | 5.40 10$^{-1}$ | $G_L$, kg m$^{-2}$ s$^{-1}$ | 5.07 10$^{-4}$ | g, m s$^{-2}$ | 98.10 10$^{-1}$ |
| $H_S$ | 2.60 10$^{-1}$ | $G_G$, kg m$^{-2}$ s$^{-1}$ | 1.74 10$^{-5}$ | $D_R$, m | 3.210 10$^{-2}$ |

## RESULTS AND DISCUSSION

Experiments were conducted at a constant liquid flow of $Q_L = 0.50\ 10^{-6}$ m$^3$ s$^{-1}$ and the gas phase was varied in the range of $Q_G = (41.69 \text{ to } 9.97)\ 10^{-6}$ m$^3$ s$^{-1}$. The mean residence times, $(t_M)_G = (t_M)_{S,G} - (t_M)_{E,G}$, were obtained from the experimental curves; $(t_M)_G$ was found to be in the range of 0.43 s to 8.47 s.

The axial dispersion coefficient and the gas-liquid and liquid-solid mass transfer coefficients were determined simultaneously by comparison between the experimental and theoretical data, obtained at the exit of the fixed bed, subject to the minimization of objective function (F) where

$$F = \sum_{k=1}^{N} \left\{ \left[\Gamma_G(1,t_A)\right]_k^{Exp} - \left[\Gamma_G(1,t_A)\right]_k^{Calc} \right\}^2 \qquad (43)$$

The initial values of $D_{ax}$, $K_{GL}$ and $k_{LS}$ were determined from the first absolute moment, $(\mu_1)_G$, of the transfer function. The first absolute moment can be related to the experimental mean residence time $(t_M)_G$ as follows:

$$(\mu_1)_G = (t_M)_G = -\frac{L}{V_{SL}} \frac{H_{d,G}}{\lim\limits_{S\to 0} \dfrac{dG^*(1,s)}{ds}} \qquad (44)$$

Development of this expression is given in Appendix D.

The numerical procedure for optimization of these parameters involved numerical inversion in the Fourier domain followed by an optimization subroutine (Cooley and Twkey, 1965; Box, 1965). The initial and optimized values of these three coefficients for differing gas - phase flow are reported below in Table 2.

In Figs. 2 and 3 results of the two sets of experiments presented show normalized profiles for concentration of gas tracer as a function of time.

A model validation process was established by comparing the theoretical results obtained with the values of the optimized parameters and the experimental data for two test cases. These results, presented in Figures 4 and 5, confirm that this reactor is represented by this model.

The axial dispersion and the interphase mass transfer phenomena characterized in the three-phase process studied are influenced by changes in gas flow. It was noted that at fixed liquid flow rates and with fixed liquid retention and partial wetting of the bed, the highest gas-liquid and liquid-solid mass transfer effects were obtained for the highest gas - phase flow. Consequently, parameters $D_{ax}$, $K_{GL}$ and $k_{LS}$ can be described by empirical correlations. Correlations taken from Stiegel and Shah (1977), Fukushima and Kusaka (1977) and Chou et al. (1979) were applied in modified form by the authors. These data were reformulated with dimensionless numbers as $Fr_G$, $We_G$ and $Sc_G$ (Table 3) and were fitted by the nonlinear least-squares method; they are restricted to the following ranges of operation: $d_P = 3.20\ 10^{-3}$ m, $21.36 \le Re_G \le 92.56$, $10^{-4} \le Fr_G \le 3.23\ 10^{-3}$, $5.30\ 10^{-2} \le Sc_G \le 2.28\ 10^{-1}$ and $10^{-5} \le We_G \le 8.30\ 10^{-4}$.

Figs. 6, 8 and 10 show plots of $D_{ax}$, $K_{GL}$ and $k_{LS}$ as a function of $Re_G$, $Fr_G$, $Sc_G$ and $We_G$. Figs. 7, 9 and 11 contain parity plots of the results obtained through the method applied in this work for each gas flow utilized in the three-phase operation vs those results predicted from the correlations expressed by Eqs. 45, 46 and 47.

**Table 2: Initial and optimized values of the dispersion coefficient and mass transfer parameters. $Q_L = 0.50\ 10^{-6}\ m^3\ s^{-1}$ .**

| Gas - Phase Flows | Initial Values | | | Optimized Values | | | Objective Function |
|---|---|---|---|---|---|---|---|
| $Q_G\ 10^6$ ($m^3\ s^{-1}$) | $D_{ax}\ 10^5$ ($m^2\ s^{-1}$) | $K_{GL}\ 10^4$ ($m\ s^{-1}$) | $k_{LS}\ 10^2$ ($m\ s^{-1}$) | $D_{ax}\ 10^5$ ($m^2\ s^{-1}$) | $K_{GL}\ 10^4$ ($m\ s^{-1}$ | $k_{LS}\ 10^2$ ($m\ s^{-1}$) | F $10^4$ |
| 41.69 | 63.89 | 69.33 | 49.18 | 33.95 | 37.79 | 20.43 | 1.57 |
| 40.00 | 59.29 | 63.91 | 45.20 | 32.78 | 36.89 | 19.23 | 1.47 |
| 38.35 | 56.07 | 57.43 | 41.77 | 31.19 | 35.14 | 18.01 | 1.40 |
| 36.68 | 49.12 | 56.98 | 39.20 | 29.98 | 34.24 | 16.89 | 1.41 |
| 35.01 | 48.02 | 50.43 | 36.14 | 28.40 | 32.57 | 15.52 | 1.37 |
| 33.34 | 45.27 | 49.10 | 31.21 | 27.23 | 31.69 | 13.31 | 1.39 |
| 31.67 | 40.98 | 47.35 | 29.06 | 25.66 | 30.12 | 11.92 | 1.21 |
| 30.01 | 39.01 | 44.12 | 26.98 | 24.47 | 29.13 | 10.14 | 1.38 |
| 28.34 | 37.40 | 41.09 | 21.15 | 22.88 | 27.58 | 9.39 | 1.12 |
| 26.67 | 36.14 | 39.12 | 19.51 | 21.67 | 26.77 | 8.23 | 1.21 |
| 25.01 | 34.21 | 35.42 | 13.78 | 20.11 | 25.14 | 6.87 | 1.30 |
| 23.33 | 33.14 | 31.77 | 10.27 | 18.95 | 24.17 | 5.46 | 1.09 |
| 21.66 | 29.20 | 29.10 | 9.08 | 17.40 | 22.46 | 4.39 | 1.27 |
| 19.99 | 27.12 | 27.81 | 7.29 | 16.23 | 21.55 | 3.02 | 1.16 |
| 18.32 | 24.01 | 23.18 | 5.21 | 14.67 | 19.88 | 2.06 | 1.01 |
| 16.65 | 21.14 | 21.14 | 4.20 | 13.46 | 18.93 | 1.54 | 1.11 |
| 14.98 | 18.22 | 19.88 | 3.02 | 11.89 | 17.22 | 0.97 | 1.21 |
| 13.31 | 16.10 | 18.10 | 2.51 | 10.71 | 16.23 | 0.78 | 1.17 |
| 11.64 | 11.89 | 16.80 | 2.01 | 9.09 | 14.54 | 0.48 | 1.18 |
| 9.97 | 9.78 | 13.98 | 1.09 | 7.89 | 13.65 | 0.27 | 1.08 |

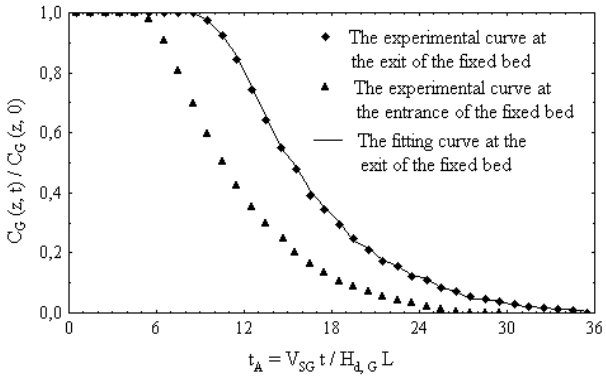


**Figure 2:** Concentration profiles for the methane gas tracer at the entrance and the exit of the γ - $Al_2O_3$ bed in $Q_G = 33.34\ 10^{-6}\ m^3\ s^{-1}$ and $Q_L = 0.50\ 10^{-6}\ m^3\ s^{-1}$

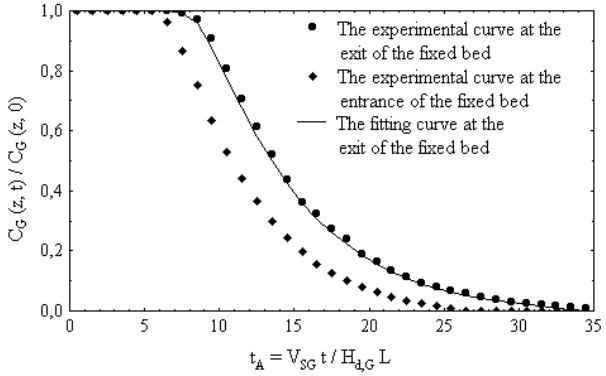


**Figure 3:** Concentration profiles for the methane gas tracer at the entrance and the exit of the γ - $Al_2O_3$ bed in $Q_G = 18.32\ 10^{-6}\ m^3\ s^{-1}$ and $Q_L = 0.50\ 10^{-6}\ m^3\ s^{-1}$

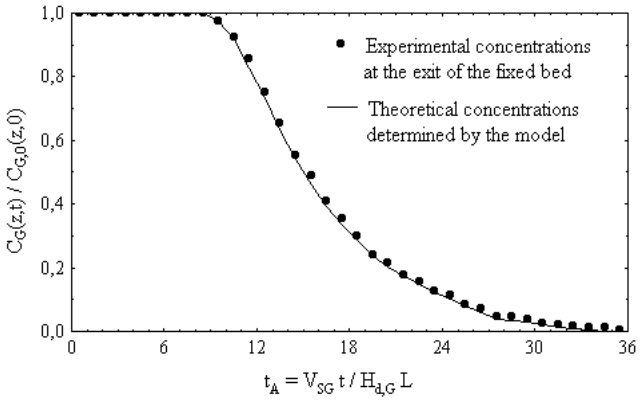


**Figure 4:** Validation of the tracer concentration at the exit of the γ-$Al_2O_3$ bed; ♦ results in gas and liquid flows $Q_G = 36.68\ 10^{-6} m^3\ s^{-1}$ and $Q_L = 0.5\ 10^{-6} m^3\ s^{-1}$; — results in parameters $D_{ax} = 2.98\ 10^{-4}\ m^2 s^{-1}$, $K_{GL} = 3.24\ 10^{-3}\ m\ s^{-1}$ and $k_{LS} = 1.68\ 10^{-1}\ m\ s^{-1}$

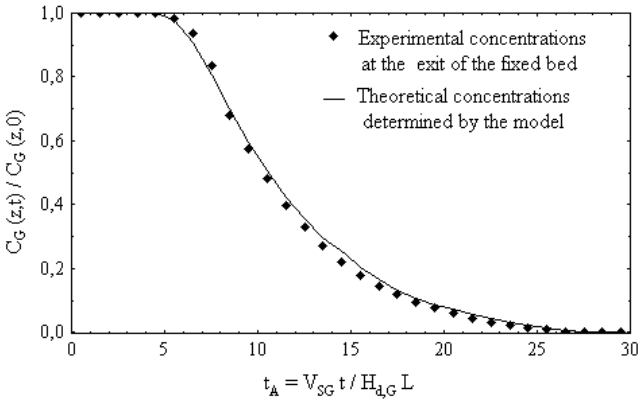


**Figure 5:** Validation of the tracer concentration at the exit of the γ-$Al_2O_3$ bed; ♦ results in gas and liquid flows $Q_G = 14.98\ 10^{-6} m^3\ s^{-1}$ and $Q_L = 0.5\ 10^{-6} m^3\ s^{-1}$; — results in parameters $D_{ax} = 1.18\ 10^{-4}\ m^2 s^{-1}$, $K_{GL} = 1.72\ 10^{-3}\ m\ s^{-1}$ and $k_{LS} = 1.56\ 10^{-2}\ m\ s^{-1}$

**Table 3: Correlations for axial dispersion and mass transfer parameters.**

| Correlations | Statistical Results | References |
|---|---|---|
| $D_{ax} = 1.67\ 10^{-6} (Re_G)^{0.088} (Fr_G)^{0.432}$ (45) | $(\sigma)_{Dax} = 8.09\ 10^{-5}$ R = 0.9942 | Stiegel and Shah (1977) |
| $K_{GL} = 1.65\ 10^{-4} (Re_G)^{-0.842} (We_G)^{-1.576}$ (46) | $(\sigma)_{KGL} = 7.60\ 10^{-5}$ R = 0.9945 | Fukushima and Kusaka (1977) |
| $k_{LS} = 3.58\ 10^{-3} (Re_G)^{1.397} (Sc_G)^{0.317}$ (47) | $(\sigma)_{kLS} = 0.0672$ R = 0.9917 | Chou et al. (1979) |

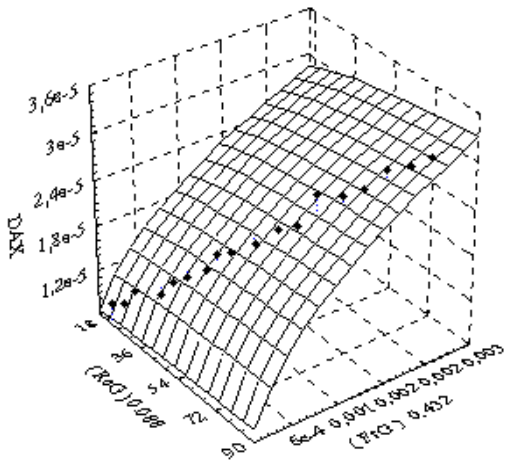


**Figure 6:** $D_{ax}$ vs $(Re_G)^{0.088}$, $(Fr_G)^{0.432}$ for the $H_2O/Ar - CH_4/\gamma - Al_2O_3$ system in trickle-bed regime

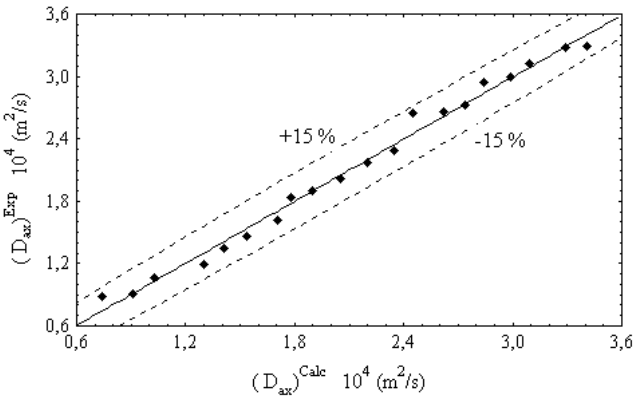


**Figure 7:** $(D_{ax})^{Exp}$ vs $(D_{ax})^{Calc}$ for the $H_2O/Ar - CH_4/\gamma - Al_2O_3$ system in trickle-bed regime. $Q_G$ = (41.69 to 9.97) $10^{-6}\ m^3\ s^{-1}$ and $Q_L = 0.50\ 10^{-6}\ m^3\ s^{-1}$

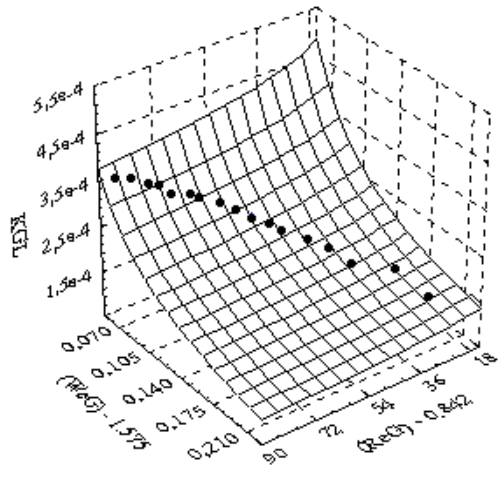


**Figure 8:** $K_{GL}$ vs $(Re_G)^{-0.842}$, $(We_G)^{-1.576}$ for the $H_2O/Ar - CH_4/\gamma - Al_2O_3$ system in trickle-bed regime

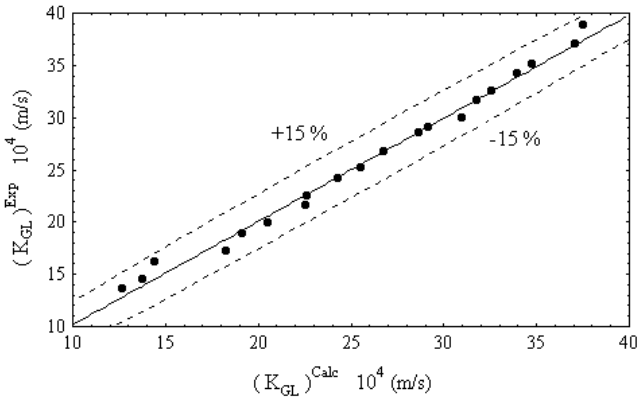


**Figure 9:** $(K_{GL})^{Exp}$ vs $(K_{GL})^{Calc}$ for the $H_2O/Ar - CH_4/\gamma - Al_2O_3$ system in trickle-bed regime. $Q_G$ = (41.69 to 9.97) $10^{-6}$ $m^3$ $s^{-1}$ and $Q_L$ = 0.50 $10^{-6}$ $m^3$ $s^{-1}$

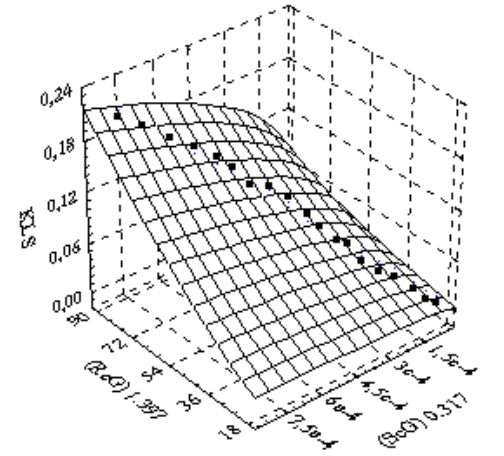


**Figure 10:** $k_{LS}$ vs $(Re_G)^{1.397}$, $(Sc_G)^{0.317}$ for the $H_2O/Ar - CH_4/\gamma - Al_2O_3$ system in trickle-bed regime

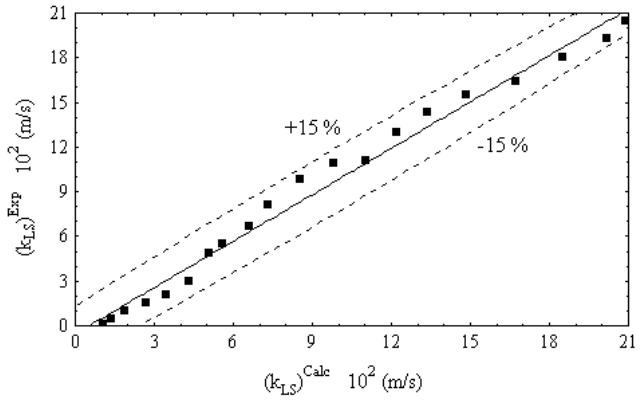


**Figure 11:** $k_{LS, Exp}$ vs $k_{LS, Calc}$ for the $H_2O/Ar - CH_4/\gamma - Al_2O_3$ system in trickle-bed regime. $Q_G$ = (41.692 to 9.973) $10^{-6}$ $m^3$ $s^{-1}$ and $Q_L$ = 0.50 $10^{-6}$ $m^3$ $s^{-1}$

## CONCLUSIONS

Based on the experimental and modeling studies of this gas-phase trickle-bed systems the following results were obtained: (i) estimation of parameters $D_{ax}$, $K_{GL}$ and $k_{LS}$, (ii) validation of the model and (iii) analysis of the behavior of the axial dispersion and gas-liquid and liquid-solid coefficients by new forms of empirical correlations.

The final values of the parameters were obtained with values of the objective function, F = 1.08 $10^{-4}$ to 1.57 $10^{-4}$. Thus, the range of optimized values of the parameters obtained by the fitting between the experimental and theoretical response and according to validation tests are given as $D_{ax}$ = 33.95 $10^{-5}$ $m^2$ $s^{-1}$ to 7.89 $10^{-5}$ $m^2$ $s^{-1}$, $K_{GL}$ = 37.79 $10^{-4}$ m $s^{-1}$ to 13.65 $10^{-4}$ m $s^{-1}$ and $k_{LS}$ = 20.43 $10^{-2}$ m $s^{-1}$ to 0.27 $10^{-2}$ m $s^{-1}$.

## ACKNOWLEDGMENTS

The authors would like to thank CNPq (Conselho Nacional de Desenvolvimento Científico e Tecnológico) for its financial support (process 141496/98-3).

## NOMENCLATURE

$a_1(s)$ Function defined in Eq. 28
$a_{GL}$ Gas-liquid mass transfer area per unit

column volume [$m^{-1}$]

$a_P$ Effective liquid-solid mass transfer area per unit column volume [$m^{-1}$]

$C_{G,0}$ Input concentration of the gas tracer [kg $m^{-3}$]

$C_G(z,t)$ Concentration of the gas tracer in the gaseous phase [kg $m^{-3}$]

$C_L(z,t)$ Concentration of the $CH_4$ tracer in the liquid phase [kg $m^{-3}$]

$C_r(r,t)$ Concentration of the $CH_4$ tracer in the solid phase [kg $m^{-3}$]

D(s) Determinant defined in Appendix C, Eq.C9

$D_i(s)$ Determinant defined in Appendix C, i = 1, 2, 3

$D_{ax}$ Axial dispersion coefficient for the gas tracer in the liquid phase [$m^2$ $s^{-1}$]

$D_e$ Effective diffusivity for the gas tracer in the solid phase [$m^2$ $s^{-1}$]

$d_h$ Equivalent diameter of the bed, $d_h = d_P [16 (\varepsilon_{ex})^2 / 9 \pi (1 - \varepsilon_{ex})^2 ]^{1/3}$ [m]

$D_p$ Diameter of the catalyst particle [m]

$D_r$ Diameter of the reactor [m]

F Objective function

$f_i(s)$ Integration constants; i = 1, 2, 3

$f_e$ Partial wetting factor

$Fr_G$ Modified Froude number, $Fr_G = \rho_G (V_{SG})^2 / d_h (\rho_G g + \delta_{GL})$

g Standard acceleration of gravity [m $s^{-2}$]

$G_G$ Mass velocity of the gaseous phase [kg $m^{-2}s^{-1}$]

$G_L$ Mass velocity of the liquid phase [kg $m^{-2}s^{-1}$]

H Solubility constant of Henry's law, dimensionless

H(s) Function defined in Eq. 35

$H_{d,G}$ Dynamic gas holdup, dimensionless

$H_{d,L}$ Dynamic liquid holdup, dimensionless

$H_S$ Static liquid holdup, dimensionless

i complex number $\sqrt{-1}$

J(s) Function defined in Eq. 35

$K_i(s)$ Function defined in Eq. 31, i = 1, 2

$K_i$ Constants defined in Eq. 9, i = 1, 2

$K_A$ Adsorption equilibrium constant [$m^3$ $kg^{-1}$]

$K_{GL}$ Overall gas-liquid mass transfer coefficient [m $s^{-1}$]

$k_{LS}$ Liquid-solid mass transfer coefficient [m $s^{-1}$]

L Height of the catalyst bed [m]

P Pressure [Pa]

$P_E^*$ Modified Peclet number based on the height of the catalyst bed

$P_E$ Peclet number based on the height of the catalyst bed

Q(s) Function defined in Eq. 36

$Q_G$ Flow of the gaseous phase [$m^3$ $s^{-1}$]

$Q_L$ Flow of the liquid phase [$m^3$ $s^{-1}$]

r Radial distance in the catalyst particle bed [m]

R Radius of the catalyst particle [m]

R(s) Function defined in Eq. 28

$Re_G$ Reynolds number, $Re_G = V_{SG} \rho_G d_h / \mu_G$

Sh Sherwood number, $Sh = k_{LS} R / D_e$

$Sc_G$ Schmidt number, $Sc_G = \mu_G / \rho_G D_{ax}$

t Time (s)

T Temperature of the system [ K ]

T(s) Function defined in Eq. 36

$t_A$ Dimensionless time defined in Eq. 10

$(t_M)_G$ Mean residence time [s]

$V_i^*$ Function defined in Appendix C, i = 1, 2, 3

$V_R$ Volume of the reactor [$m^3$]

$V_{SG}$ Superficial velocity of the gaseous phase [m $s^{-1}$]

$V_{SL}$ Superficial velocity of the liquid phase [m $s^{-1}$]

$We_G$ Weber number, $We_G = (V_{SG})^2 \rho_G d_h / \sigma_L$

W Catalytic mass, kg

z Axial distance of the catalytic reactor [m]

### *Greek Letters*

$\alpha$ Parameter defined in Eq.17, dimensionless

$\beta$ Angle for the vertical inclination defined in Eq. 7

$\gamma$ Parameter defined in Eq.17, dimensionless

$\Gamma_i$ Dimensionless concentrations of the gas, liquid and solid, i = G, L, S

$\Gamma_i^*$ Laplace domain concentrations of the gas, liquid and solid, i = G, L, S

$\delta(s)$ Function defined in Eq. 31

$\delta_{GL}$ Two-phase pressure [kg $m^{-2}$ $s^{-2}$]

$\varepsilon_{ex}$ Void fraction in the bed, dimensionless

$\eta$ Radial distance in the catalyst particle, dimensionless

$\kappa$ Parameter defined in Eq. 17

$\lambda$ Parameter defined in Eq. 18

$\lambda_i$ Roots of the characteristic Eq. 32, i = 1, 2, 3

$\mu_L$ Viscosity of the liquid phase [kg $m^{-1}$ $s^{-1}$]

$\mu_G$ Viscosity of the gaseous phase [kg $m^{-1}$ $s^{-1}$]

$\rho_G$ Density of the gaseous phase [kg $m^{-3}$]

$\rho_L$ Density of the liquid phase [kg $m^{-3}$]

$\rho_P$ Density of the particle [kg $m^{-3}$]

$\rho_{Le}$ Bed density [kg $m^{-3}$]

$\sigma_L$ Surface tension [kg $s^{-2}$]

## REFERENCES

Al–Dahhan, M.H., Larachi, F., Dudukovic, M.P. and Laurent, A., High-Pressure Trickle Bed Reactors: A Review, Industrial Engineering Chemical

Research, 36, 3292-3314 (1997).

Attou, A., Boyer, C. and Ferschneider, G., Modeling of Hydrodynamics of the Cocurrent Gas-Liquid Trickle Flow in a Trickle-Bed Reactor, Chemical Engineering Science, 54, 785-802 (1999).

Box, P., A New Method of Constrained Optimization and a Comparison with Other Methods, Computer Journal, 8, 42-52 (1965).

Burghardt, A., Kolodziej, A.S. and Zynski, J., Experimental Studies of Liquid-Solid Wetting Efficiency in Trickle-Bed Concurrent Reactors, The Chemical Engineering Journal, 28, 35-49 (1990).

Burghardt, A., Grazyna, B., Miczylaw, J. and Kolodziej, A., Hydrodynamics and Mass Transfer in a Three-Phase Fixed Bed Reactor with Cocurrent Gas-Liquid Downflow, The Chemical Engineering Journal, 28, 83-99 (1995).

Chin, D. and King, C.J., Adsorption of Glycols, Sugars and Related Multiple-OH Compounds on to Activated Carbons. 1. Adsorption Mechanisms, Industrial Engineering Chemical Research, 38, 3738-3745 (1999).

Cooley, J.W. and Twkey, J.W., An Algorithm for the Machine Calculation of Complex Fourier Series, Maths. Comp., 19, 297-301 (1965).

Chou, T.S., Worley, F.L. and Luss, D., Local Particle–Liquid Mass Transfer Fluctuations in Mixed-Phase Cocurrent Downflow Through a Fixed Bed in the Pulsing Regime, 18, 279 (1979).

Fukushima, S. and Kusaka, K., Liquid-Phase Volumetric Mass Transfer Coefficient and Boundary of Hydrodynamics Flow Region in Packed Column with Cocurrent Downward Flow, J. Chem. Eng. Japan, 10, 467-474 (1977).

Funk, G.A., Harold, M.P. and Ng, K.M., A Novel Model for Reaction in Trickle-Beds with Flow Maldistribution, Industrial Engineering Chemical Research, 29, 733-748 (1990).

Gallezot, P., Nicolaus, N., Aiche, G., Fuertes, P. and Perrard, A., Glucose Hydrogenation on Ruthenium Catalysts in a Trickle Bed Reactor, Journal of Catalysis, 180, 1-5 (1998).

Gianetto, A. and Specchia, V., Trickle-Bed Reactors: State of the Art and Perspectives, Chem. Eng. Sci., 3197-3213 (1992).

Hutton, B.E.T., Leung, L.S., Brooks, P.C. and Nicklin, D.J., On Flooding in Packed Columns, Chem. Eng. Sci. 29, 493-500 (1974).

Iliuta, I., and Thyrion, F.C., Flow Regimes, Liquid Holdups and Two-Phase Pressure Drop for Two-Phase Cocurrent Downflow and Upflow Through Packed Bed: Air/Newtonian and Non-Newtonian Liquid Systems, Chem. Eng. Sci., 52, 4045-4053 (1997).

Iliuta, I., Thyrion, F.C., Bolle, L. and Giot, M., Comparison of Hydrodynamic Parameters for Countercurrent and Cocurrent Flow Through Packed Beds, Chem. Eng. Sci., 20, 171-181, (1997).

Iliuta, I., Larachi, F. and Grandjean, B.P.A., Residence Time, Mass Transfer and Back-mixing of the Liquid in Trickle Flow Reactors Containing Porous Particles, Chem. Eng. Sci., 54, 4099-4109 (1999).

Iliuta, I., Bildea, S.C., Iliuta, M.C. and Larachi, F., Analysis of Trickle Bed and Packed Bubble Column Bioreactors for Combined Carbon Oxidation and Nitrification, Brazilian Journal of Chemical Engineering, 19, 69-87 (2002).

Jiang, Y., Khadilkar, M.R., Al-Dahhan, M.H. and Dudukovic, M.P., Two-Phase Flow Distribution 2D Trickle Bed Reactors, Chem. Eng. Sci., 54, 2409-2419 (1999).

Lamine, A.S., Gerth, L., Legall H. and Wild, G., Heat Transfer in a Packed Bed Reactor with Cocurrent Downflow of a Gas and Liquid, Chem. Eng. Sci., 51, 3813-3827 (1996).

Larachi, F., Laurent, A., Midoux, N. and Wild, G., Experimental Study of a Trickle Bed Reactor Operating at High Pressure: Two-Phase Pressure Drop and Liquid Saturation, Chem. Eng. Sci, 46, 1233-1246 (1991).

Latifi, M.A., Naderifar, A. and Midoux, N. Experimental Investigation of the Liquid-Solid Mass Transfer at the Wall of Trickle Bed – Influence of Schmidt Number, Chem. Eng. Sci., 52, 4005-4011 (1997).

Pawelec, B., Mariscal, R., Fierro,J.L.G., Greenwood, A. and Vasudevan, P.T., Carbon-Supported Tungsten and Nickel Catalysts for Hydrodesulfurization and Hydrogenation Reactions, Applied Catalysis A: General, 206, 295-307 (2001).

Pironti, F., Mizrahi, D., Acosta, A. and González-Mendizabal, D., Liquid-Solid Wetting Factor in Trickle Bed Reactors: Its Determination by a Physical Method, Chem. Eng. Sci., 54, 3793-3800 (1999).

Rajashekharam, M.V., Jaganathan, R. and Chaudhari, V., A Trickle Bed Reactor Model for Hydrogenation of 2,4 Dinitrotoluene : Experimental Verification., Chem. Eng. Sci., 53, 787-805 (1998).

Ramachandran P.A. and Chaudhari, R.B., Three Phase Catalytic Reactors, Gordan and Breach, New York, U.S.A., Chap. 7 (1983).

Ramachandran, P.A. and Smith, J., Dynamics Behavior of Trickle-Bed Reactors, Chem. Eng. Sci., 34, 75-91 (1979).

Reinecke, N., Petritsch, G., Schimitz, D. and Mewes, D., Tomographic Measurement Techniques-Visualization of Multiphase Flow, Chem. Eng. Tech, 21, 7 (1998).

Silva, J.D., Avaliação Experimental e Modelagem do Processo Gás-Líquido-Sólido em Reatores de Leito Gotejante, M.Sc. thesis, write at Federal University of Pernambuco, Recife - PE, Brazil (1996).

Silva, J.D., Lima, F.R.A. and Abreu, C.A.M., Avaliação Experimental e Simulação num Reator de Leito Gotejante Usando Traçador Gasoso, XXVII Congresso Brasileiro de Sistema Particulados, 451-458 (1999).

Silva, J.D., Lima, F.R.A. and Abreu, C.A.M., Modelagem e Simulação do Comportamento do Hidrogênio em um Reator de Leito Gotejante, XIII Congresso Brasileiro de Engenharia Química, on CD-ROM (2000a).

Silva, J.D., Lima, F.R.A. and Abreu C.A.M., Análise Dinâmica de um Reator Trifásico a Leito Fixo Gás-Líquido-Sólido com Escoamento Concorrente Descendente das Fases Gasosa e Líquida em Leito Poroso, XXVIII Congresso Brasileiro de Sistema Particulados, 121-128 (2000b).

Specchia, V. and Baldi, G., Pressure Drop and Liquid Holdup for Two Phase Concurrent Flow in Packed Beds, Chem. Eng. Sci, 32, 515-523 (1977).

Stiegel, G.J. and Shah, Y.T., Axial Dispersion in a Rectangular Bubble Column, J. Chem. Eng., 55, 3 (1977).

Toye, D., Marchot, P., Crine, M. and L'homme, G., The Use of Large-Scale Computer Assisted Tomography for The Study of Hydrodynamics in Tricking Filters, Chem. Eng. Sci., 49, 5271 (1994).

Tsamatsoulis, D. and Papayannakos, N., Simulation of Non Ideal Flow in a Trickle-Bed Hydrotreater by the Cross-Flow Model, Chem. Eng. Sci., 50, 3685-3691 (1995).

Van Der Laan, E. Th., Notes on the Diffusion-Type Model for the Longitudinal Mixing in Flow, Chem. Eng. Sci., 7, 187-191 (1957).

Wu, Y., Al-Dahhan, M.H., Khadilkar, M.R. and Dudukovic, M.R., Evaluation of Trickle-Bed Reactors Models for a Liquid Limited Reaction, Chem. Eng. Sci., 51, 2721-2725 (1996).

## APPENDIX A

Eq. 21 was solved in the following manner:

$$\frac{d^2\,\Gamma_r^*(\eta,s)}{d\eta^2}+\frac{2}{\eta}\frac{d\,\Gamma_r^*(\eta,s)}{d\eta}=\left[\phi(s)\right]^2\,\Gamma_r^*(\eta,s)\,;\qquad \left[\phi(s)\right]^2=\frac{s}{\lambda} \tag{A1}$$

A change in variable in this equation and its boundary conditions was made using the following ratio:

$$\Gamma_r^*(\eta,\ s)\ =\ \frac{P_r^*(\eta,\ s)}{\eta} \tag{A2}$$

Using the above ratio Eq. A1 was transformed into:

$$\frac{d^2P_r^*}{d\eta^2}-\left[\phi(s)\right]^2 P_r^*(\eta,s)=0 \tag{A3}$$

$$\frac{d\,P_r^*(1,s)}{d\eta}=Sh\;\Gamma_L^*(\xi,s)-(Sh-1)\,P_r^*(1,s)\,;\qquad P_r^*(0,s)=0 \tag{A4}$$

The solution of Eq. A3 with its boundary conditions given by Eq. A4 is

$$P_r^*(\eta,s)=\frac{Sh\;\Gamma_L^*(\xi,s\ )\,\mathrm{senh}\left[\ \phi(s)\ \right]\eta}{\left\{\phi(s)\cosh\left[\phi(s)\right]+(Sh-1)\,\mathrm{senh}\left[\phi(s)\right]\right\}} \tag{A5}$$

With the original variable $\Gamma^*_r(\eta, s)$, given by Eq. A2, the following equation was obtained:

$$\Gamma_r^*(1,s)=\frac{Sh\;\Gamma_L^*(\xi,s)}{\left[\phi(s)\,\coth\left[\phi(s)\right]+(Sh-1)\right]} \tag{A6}$$

## APPENDIX B

Combining Eqs. 19 and 20 in the Laplace domain,

$$\frac{d\Gamma_G^*(\xi,s)}{d\xi}+a_1(s)\Gamma_G^*(\xi,s)=\alpha\Gamma_L^*(\xi,s) \tag{B1}$$

$$\frac{1}{P_E^*}\frac{d^2\Gamma_L^*(\xi,s)}{d\xi^2}-\kappa\frac{d\Gamma_L^*(\xi,s)}{d\xi}= -\gamma\Gamma_G^*(\xi,s)+\nu(s)\Gamma_L^*(\xi,s) \tag{B2}$$

Combination 1: the response in the gaseous phase was obtained as follows**:** isolating $\Gamma^*_L(\xi,s)$ from Eq. B1 and then differentiating $\Gamma^*_L(\xi, s)$ twice with respect to $\xi$.

$$\Gamma_L^*(\xi,s)=\frac{1}{\alpha}\frac{d\Gamma_G^*(\xi,s)}{d\xi}+\frac{a_1(s)}{\alpha}\Gamma_G^*(\xi,s) \tag{B3}$$

$$\frac{d\ \Gamma_L^*(\xi,s)}{d\xi}=\frac{1}{\alpha}\frac{d^2\Gamma_G^*(\xi,s)}{d\xi^2}+\frac{a_1(s)}{\alpha}\frac{d\Gamma_G^*(\xi,s)}{d\xi} \tag{B4}$$

$$\frac{d^2\Gamma^*_L(\xi,s)}{d\xi^2}=\frac{1}{\alpha}\frac{d^3\Gamma_G^*(\xi,s)}{d\xi^3}+\frac{a_1(s)}{\alpha}\frac{d^2\Gamma_G^*(\xi,s)}{d\xi^2} \tag{B5}$$

Introducing Eq. B3, B4 and B5 in to Eq. B2, the following equation for the methane gas tracer in the gaseous phase was found:

$$\frac{d^3\Gamma_G^*(\xi,s)}{d\xi^3}+\delta(s)\frac{d^2\Gamma_G^*(\xi,s)}{d\xi^2} -K_1(s)\frac{d\Gamma_G^*(\xi,s)}{d\xi}+K_2(s)\,\Gamma_G^*(\xi,s)=0 \tag{B6}$$

where

$$\delta(s)=\left[a_1(s)-P_E^*\kappa\right];$$

$$K_1(s)=\left[a_1(s)\kappa+\nu(s)\right]P_E^*; \tag{B7}$$

$$K_2(s)=\left[\alpha\gamma-a_1(s)\nu(s)\right]P_E^*$$

Combination 2: The response in the liquid phase was obtained as follows: isolating $\Gamma^*_G(\xi, s)$ from Eq. B2 and then differentiating $\Gamma^*_G(\xi, s)$ with respect to $\xi$.

$$\Gamma_G^*(\xi,s)=-\frac{1}{P_E^*\gamma}\frac{d^2\Gamma_L^*(\xi,s)}{d\xi^2} +\frac{\kappa}{\gamma}\frac{d\Gamma_L^*(\xi,s)}{d\xi}+\frac{\nu(s)}{\gamma}\Gamma_L^*(\xi,s) \tag{B8}$$

$$\frac{d\Gamma_G^*(\xi,s)}{d\xi}=-\frac{1}{P_E^*\gamma}\frac{d^3\Gamma_L^*(\xi,s)}{d\xi^3} +\frac{\kappa}{\gamma}\frac{d^2\Gamma_L^*(\xi,s)}{d\xi^2}+\frac{\nu(s)}{\gamma}\frac{d\ \Gamma_L^*(\xi,s)}{d\xi} \tag{B9}$$

Eqs. B8 and B9 were introduced in to Eq. B1 to obtain the following equation:

$$\frac{d^3\Gamma_L^*(\xi,s)}{d\xi^3}+\delta(s)\frac{d^2\Gamma_L^*(\xi,s)}{d\ \xi^2} -K_1(s)\frac{d\Gamma_L^*(\xi,s)}{d\xi}+K_2(s)\Gamma_L^*(\xi,s)=0 \tag{B10}$$

## APPENDIX C

Formal solutions of Eqs. B6 and B10 were suggested by Ramachandran and Smith (1979), as follows:

$$\Gamma_G^*(\xi,s)=\sum_{i=1}^{3}f_i(s)\exp\left[\lambda_i(s)\right];$$

$$\Gamma_L^*(\xi,s)=\sum_{i=1}^{3}\left[\lambda_i(s)-a_1(s)\right]\frac{f_i(s)}{\alpha}\exp\left[\lambda_i(s)\right] \tag{C1}$$

In Eq. C1 the integration constants, $f_i(s)$, were calculated from the three boundary conditions given in Eqs. 22 and 23**,** expressed in the Laplace domain. They were evaluated by the following system of algebraic equations:

$$f_1(s)+f_2(s)+f_3(s)=1/s \tag{C2}$$

$$\left\{\left[\lambda_1(s)-a_1(s)\right]\lambda_1(s)\exp\left[\lambda_1(s)\right]\right\}f_1(s)+\left\{\left[\lambda_2(s)-a_1(s)\right]\lambda_2(s)\exp\left[\lambda_2(s)\right]\right\}f_2(s)+\left\{\left[\lambda_3(s)-a_1(s)\right]\lambda_3(s)\exp\left[\lambda_3(s)\right]\right\}f_3(s)=0 \tag{C3}$$

$$\left\{\left[\lambda_1(s)-a_1(s)\right]\left[\frac{\lambda_1(s)}{P_E}-1\right]\right\}f_1(s)+\left\{\left[\lambda_2(s)-a_1(s)\right]\left[\frac{\lambda_2(s)}{P_E}-1\right]\right\}f_2(s)+\left\{\left[\lambda_3(s)-a_1(s)\right]\left[\frac{\lambda_3(s)}{P_E}-1\right]\right\}f_4(s)=0 \tag{C4}$$

The system of algebraic equations given by Eqs. (C2), (C3) and (C4) was solved by Cramer's method, so determinants D(s) were defined by

$$D(s)=T_1^*\left[\lambda_1(s),\lambda_2(s),a_1(s)\right]+T_2^*\left[\lambda_1(s),\lambda_2(s)\lambda_3(s),a_1(s)\right]+T_3^*\left[\lambda_1(s),\lambda_2(s),\lambda_3(s),a_1(s)\right] \tag{C5}$$

where

$$T_1^*\left[\lambda_1(s),\lambda_2(s),a_1(s)\right]=\left[\lambda_2(s)-a_1(s)\right]\lambda_2(s)\exp\left[\lambda_2(s)\right]\left\{\left\{\left[\lambda_2(s)-a_1(s)\right]\left[\lambda_2(s)/P_E-1\right]\right\}\left\{\left[\lambda_1(s)-a_1(s)\right]\left[\lambda_1(s)/P_E-1\right]\right\}\right\} \tag{C6}$$

$$T_2^*\left[\lambda_1(s),\lambda_2(s),\lambda_3(s),a_1(s)\right]=\left[\lambda_1(s)-a_1(s)\right]\lambda_1(s)\exp\left[\lambda_1(s)\right]\left\{\left\{\left[\lambda_2(s)-a_1(s)\right]\left[\lambda_2(s)/P_E-1\right]\right\}-\left\{\left[\lambda_2(s)-a_1(s)\right]\left[\lambda_2(s)/P_E-1\right]\right\}\right\} \tag{C7}$$

$$T_3^*\left[\lambda_1(s),\lambda_2(s),\lambda_3(s),a_1(s)\right]=\left\{\left[\lambda_3(s)-a_1(s)\right]\lambda_3(s)\exp\left[\lambda_3(s)\right]\left\{\left\{\left[\lambda_1(s)-a_1(s)\right]\left[\lambda_1(s)/P_E-1\right]\right\}-\left\{\left[\lambda_2(s)-a_1(s)\right]\left[\lambda_2(s)/P_E-1\right]\right\}\right\}\right. \tag{C8}$$

Determinants $D_1(s)$, $D_2(s)$ and $D_3(s)$ are given by

$$D_1(s)=1/s\,V_1^*\left[\lambda_2(s),\lambda_3(s),a_1(s)\right] \tag{C9}$$

$$D_2(s)=1/s\,V_2^*\left[\lambda_1(s),\lambda_3(s),a_1(s)\right] \tag{C10}$$

$$D_3(s)=1/s\,V_3^*\left[\lambda_1(s),\lambda_2(s),a_1(s)\right] \tag{C11}$$

where

$$V_1^*\left[\lambda_2(s),\lambda_3(s),a_1(s)\right]=\left[\lambda_2(s)-a_1(s)\right]\left[\lambda_3(s)-a_1(s)\right]\left\{\left[\lambda_3(s)/P_E-1\right]\lambda_2(s)\exp\left[\lambda_2(s)\right]-\left[\lambda_2(s)/P_E-1\right]\lambda_3(s)\exp\left[\lambda_3(s)\right]\right\} \tag{C12}$$

$$V_2^*\left[\lambda_1(s),\lambda_3(s),a_1(s)\right]=\left[\lambda_1(s)-a_1(s)\right]\left[\lambda_3(s)-a_1(s)\right]\left\{\left[\lambda_1(s)/P_E-1\right]\lambda_3(s)\exp\left[\lambda_3(s)\right]-\left[\lambda_3(s)/P_E-1\right]\lambda_1(s)\exp\left[\lambda_1(s)\right]\right\} \tag{C13}$$

$$V_3^*\left[\lambda_1(s),\lambda_2(s),a_1(s)\right]=\left[\lambda_1(s)-a_1(s)\right]\left[\lambda_2(s)-a_1(s)\right]\left\{\left[\lambda_2(s)/P_E-1\right]\lambda_1(s)\exp\left[\lambda_1(s)\right]-\left[\lambda_1(s)/P_E-1\right]\lambda_2(s)\exp\left[\lambda_2(s)\right]\right\} \tag{C14}$$

The integration constants are obtained as

$$f_i(s)=\frac{D_i(s)}{D(s)},\ (i=1,2,3) \tag{C15}$$

## APPENDIX D

Variables $V_1^*$, $V_2^*$ and $V_3^*$ in the transfer function are functions of $\lambda_i(s) \rightarrow i = 1, 2, 3$ and $a_1(s)$, while variables $T_1^*$, $T_2^*$ and $T_3^*$ in D(s) are also functions of $\lambda_i(s) \rightarrow i = 1, 2, 3$ and $a_1(s)$. A detailed development is given in Appendix C. The parameter estimation technique by the method of moments was developed by Van Der Laan (1957). This technique was used for parameters that are functions of the Laplace transform variable ($s \rightarrow 0$), according to the procedure below.

$$\lim_{S\to0}G^*(1,s)=\frac{1}{\lim_{S\to0}D(s)}\left\{\lim_{S\to0}\left[V_1^*\left(\lambda_2(s),\lambda_3(s),a_1(s)\right)\exp\lim_{S\to0}\lambda_1(s)\right]+\lim_{S\to0}\left[V_2^*\left(\lambda_1(s),\lambda_3(s),a_1(s)\right)\exp\lim_{S\to0}\lambda_2(s)\right]+\lim_{S\to0}\left[V_3^*\left(\lambda_1(s),\lambda_3(s),a_1(s)\right)\exp\lim_{S\to0}\lambda_3(s)\right]\right\} \tag{D1}$$

$$\lim_{S\to0}D(s)=\lim_{S\to0}T_1^*\left[\lambda_1(s),\lambda_2(s),a_1(s)\right]+\lim_{S\to0}T_2^*\left[\lambda_1(s),\lambda_2(s),\lambda_3(s),a_1(s)\right]+\lim_{S\to0}T_3^*\left[\lambda_1(s),\lambda_2(s),\lambda_3(s),a_1(s)\right] \tag{D2}$$

The term referring to the differentiation is given by the following equation:

$$\lim_{S\to0}\frac{dG^*(1,s)}{ds}=\lim_{S\to0}A_1(s)+\lim_{S\to0}A_2(s)+\lim_{S\to0}A_3(s) \tag{D3}$$

where

$$\lim_{S\to0}A_1(s)=\frac{1}{\lim_{S\to0}\left[D(s)\right]^2}\left\{\lim_{S\to0}\frac{d}{ds}\left[V_1^*\left(\lambda_2(s),\lambda_3(s),a_1(s)\right)\exp\lambda_1(s)\right]\lim_{S\to0}D(s)-\lim_{S\to0}\frac{dD(s)}{ds}\lim_{S\to0}\left[V_1^*\left(\lambda_2(s),\lambda_3(s),a_1(s)\right)\exp\lambda_1(s)\right]\right\} \tag{D4}$$

$$\lim_{S\to0}A_2(s)=\frac{1}{\lim_{S\to0}\left[D(s)\right]^2}\left\{\lim_{S\to0}\frac{d}{ds}\left[V_2^*\left(\lambda_1(s),\lambda_3(s),a_1(s)\right)\exp\lambda_2(s)\right]\lim_{S\to0}D(s)-\lim_{S\to0}\frac{dD(s)}{ds}\lim_{S\to0}\left[V_2^*\left(\lambda_1(s),\lambda_3(s),a_1(s)\right)\exp\lambda_2(s)\right]\right\} \tag{D5}$$

$$\lim_{S\to0}A_3(s)=\frac{1}{\lim_{S\to0}\left[D(s)\right]^2}\left\{\lim_{S\to0}\frac{d}{ds}\left[V_3^*\left(\lambda_1(s),\lambda_2(s),a_1(s)\right)\exp\lambda_3(s)\right]\lim_{S\to0}D(s)-\lim_{S\to0}\frac{dD(s)}{ds}\lim_{S\to0}\left[V_3^*V_3^*\left(\lambda_1(s),\lambda_2(s),a_1(s)\right)\exp\lambda_3(s)\right]\right\} \tag{D6}$$

As the differentiations of the determinants are very lengthy, they are not shown.